Proceedings of the Combustion Institute 40 (2024) 105273

Contents lists available at ScienceDirect

Proceedings of the Combustion Institute

journal homepage: www.elsevier.com/locate/proci

LES of turbulent partially-premixed flames using reaction–diffusion manifold-reduced chemistry with a consistent gradient estimate determined *"on the fly"*

Prashant Shrotriya *, Robert Schießl, Viatcheslav Bykov, Ulrich Maas

Institute of Technical Thermodynamics, Karlsruhe Institute of Technology, Engelbert-Arnold-Str. 4, Karlsruhe 76131, Germany

ARTICLE INFO

Keywords:
REDIM
Scalar-gradient correlation
Turbulent combustion
Partially-premixed flame
Large eddy simulation

ABSTRACT

This paper devises and applies a method for determining consistent, system-adapted reaction–diffusion manifolds (REDIM) for turbulent partially-premixed combustion. The method is an extension of a previous technique which was limited to laminar flames. It adapts a REDIM to the scalar gradients present in a given reacting flow by an iterative procedure, in which gradients from REDIM-reduced simulations are used to create a new and improved REDIM. An application of the method is demonstrated using large eddy simulations (LES) of a turbulent partially-premixed methane/air flame as the "gradient estimate generating" flame simulation. Compared to the previous laminar flame studies, the turbulent flame features less sharp gradient-scalar correlations because of the strong scattering of data. Methods for capturing the scatter in scalar-gradient correlations are applied, allowing us to assess the influence of the scatter on the resulting REDIM. Also, the fact that turbulent flame simulations often involve spatial filtering operations which tend to reduce the magnitude of the gradients is taken into account by comparing the REDIM output to quasi-direct numerical simulation (qDNS) data. It is found that the gradients devised from the filtered simulations are by a factor of 2–3 below those of the more fully resolved qDNS. Nevertheless, the REDIM devised from the LES predicts the states of the qDNS with good accuracy. Overall, observations show that the method can produce realistic reduced models also for systems with complex interactions of chemical reaction, molecular transport and flow, like partially-premixed turbulent flames.

1. Introduction

Partially-premixed combustion (PPC) has drawn attention in recent years, see the review by Masri [1]. Combustion models for "single-mode" combustion (*i.e.*, purely premixed or purely non-premixed) need to be extended to also cover PPC.

Large eddy simulation (LES) can cover local extinction and re-ignition, which appear in PPC, at low computational cost [2–5]. In the last decade, different sub-grid scale (SGS) combustion models for LES in combination with a reduced chemistry description have been developed [1,6–8]. Perry et al. [7] used two mixture fractions to consider the multi-stream mixing problem. Kleinheinz et al. [8] used a multi-regime combustion model where the contribution of premixed and non-premixed manifolds is accounted for in the progress variable source term.

In different models developed for PPC using flamelet-based model reduction approaches [4,8,9], it was observed that the single-mode flamelet approaches possess limitations in PPC. It is because of the different governing physics of non-premixed and premixed combustion, where diffusive time scales are rate controlling in non-premixed combustion whereas transport and chemical time scales are of the same order of magnitude in premixed combustion [3]. Therefore, different modifications in the flamelet-based techniques have been proposed, for example, blending of manifolds using flame regime indicators [4, 10]. These modifications improved single-mode-based models; however, in these blending of manifolds techniques, identification of the combustion mode is still a challenging task [11].

Reaction–diffusion manifolds (REDIM), an extension of the intrinsic low-dimensional manifold (ILDM) method [12], is another model reduction technique [13–15]. It is a generalized approach is based on a pre-defined correlation between scalars and their spatial gradients (the gradient estimates) as an input to generate a reduced model. The reduced model will represent the actual physical combustion system if the supplied gradient estimate reflects the actual scalar-gradient correlation with coupled relatively slow chemical reaction modes for

* Corresponding author.
E-mail address: prashant.shrotriya@kit.edu (P. Shrotriya).

https://doi.org/10.1016/j.proci.2024.105273
Received 4 December 2023; Accepted 31 May 2024
Available online 24 June 2024

a given combustion system, *e.g.*, for a given configuration and regime considered. The basic assumption of the time scale separation [12] guarantees that the decoupled fast modes will drive the relaxation towards the REDIM where the interplay between relatively slow chemical processes and diffusion can be fully described and sustained.

In previous work, a method for automatically inferring system-adapted gradient estimates for the REDIM was described and applied to laminar combustion systems [15,16]. Here, in a coupled approach, the REDIM model interacts with a reduced flame simulation: A flame simulation is provided with a REDIM made with gradient estimates based on the data from the flame simulation. It was found that the flame simulations using these system-adapted REDIMs were in good agreement with fully detailed calculations [15,16].

In this work, this method is extended to obtain the gradient estimates for turbulent PPC systems. It is shown that, compared to the laminar case, the process of extracting gradient estimates from the flame simulations is more challenging. For instance, scalar-gradient correlations for turbulent flames tend to be less sharp than for their laminar counterparts. Dedicated methods for assessing the influence of the unsharpness on the reduced model are described. Their application shows that the method originally applied and tested for laminar flames is successful also for turbulent flames.

The flame simulation part in the coupling is done by an LES using the well-known dynamic thickened flame (DTF) modeling approach [17–19] with REDIM-reduced chemistry, *i.e.*, DTF-REDIM SGS combustion model.

The main objectives of this paper are:

- to investigate turbulent partially-premixed flames with REDIM because REDIM does not depend upon specific flamelet scenarios and a more generalized methodology can be developed to reduce mixed-mode combustion system using REDIM;
- validate the iterative methodology for REDIM generation in unsteady situations (where a very high range of scattering in the gradient field is observed) with experimental and quasi-direct numerical simulation (qDNS) datasets.

2. Test configuration

For the simulation validation, the FJ200-5GP-Lr75-57 flame case from the experimental database jointly provided by the University of Sydney and Sandia National Laboratory is considered. It is chosen because its inhomogeneous CH_4/air mixture inlet conditions lead to PPC [20]. A highly resolved and model-free qDNS for that flame has been performed by Zirwes et al. [21]. Since the grid resolution achieves direct numerical simulations (DNS) quality only in upstream locations, where experimental data are available, and the second-order discretization schemes were used, they used the term qDNS [21]. This setup has a main jet coming from a cylindrical mixing chamber. The mixing chamber has concentric circular nozzles, where in the inner and the outer nozzles, fuel and air streams flow, respectively. The length of the mixing chamber can be varied by changing the recession length (L_r) of the inner fuel nozzle from the main jet exit. The mixing tube is surrounded by a pilot flow of a mixture of C_2H_2, H_2, CO_2, N_2 and air in proper proportion to match the equilibrium gas temperature and composition of stoichiometric CH_4/air. The main jet surrounded by the pilot enters the wind tunnel where co-flow air is supplied. A detailed description of the configuration can be found in [20].

3. Modeling approach

3.1. Overview of REDIM method

The REDIM method provides a simplified description of the dynamics in reactive–diffusive systems in terms of a set of a few reduced variables. It has been described in previous papers [13–16], so only a short description is provided here. The thermo-kinetic state vector ψ (consisting, for instance, of specific enthalpy, pressure and species) in the transport equation for a reacting flow is assumed to be dependent on a small number (typically, 1–3) of reduced variables, θ. A REDIM is uniquely determined by a detailed reaction mechanism and data for molecular transport, boundary conditions and the gradient estimate. The latter expresses the spatial gradients of the reduced variables $\mathrm{grad}\theta$ as a function $\chi(\theta)$ of the reduced variables. This function characterizes how the (gradient-driven) diffusive fluxes depend on the states, and it can be used to adapt the REDIM to a given combustion system [13].

3.2. REDIM implementation in reduced calculations

If the gradient estimate of the REDIM is taken as a free (function-valued) parameter, rather than an *a priori* given function, the states on the REDIM become dependent on both the set of reduced variables θ and on the gradient estimate $\chi(\theta)$, *i.e.*, $\psi = \psi(\theta; \chi(\theta))$. Recently, a technique for creating a REDIM with a system-adapted gradient estimate has been demonstrated for laminar flames [15,16]. Formally, denoting with $\mathcal{M}_{\chi_a}$ the REDIM that results for the given gradient estimate χ_a, the method starts with a simple first guess χ_0 for the gradient estimates to create a REDIM $\mathcal{M}_{\chi_0}$. Next, $\mathcal{M}_{\chi_0}$ is used as the chemistry model in a flame simulation, which yields information on the spatial gradients of the reduced variables $\nabla\theta(x)$. These new gradient estimates $\chi_1(\theta)$ are inferred from $\nabla\theta(x)$; this gradient estimate extraction from empirical data is briefly described in the next subsection. A detailed explanation of this method is provided in [16]. From the $\chi_1(\theta)$, the corresponding REDIM $\mathcal{M}_{\chi_1}$ is computed. These steps are repeated, producing an improved gradient estimate $\chi_{n+1}(\theta)$ from the previous $\chi_n(\theta)$ in each iteration, until the residual $\chi_{n+1}(\theta) - \chi_n(\theta)$ (and, by continuity of the dependence of the REDIM on the gradient estimates, also the residual $\mathcal{M}_{\chi_{n+1}} - \mathcal{M}_{\chi_n}$) converges.

As suggested in [16], this method can be used for inferring system-adapted gradient estimates $\chi(\theta)$. However, implementing the method is not straightforward, especially in the case of turbulent combustion. Several challenges need to be addressed, namely:

- scatter: in turbulent flames, the correlation between gradients and scalars is not as sharp as in laminar flames;
- filtering: turbulent flame simulations often involve some spatial filtering or averaging operations; the gradients obtained by these simulations therefore do not necessarily represent the actual gradients in the reacting flow.

Now we describe step by step the proposed implementation, including the modifications required to address the turbulent case. The spatial gradients $\nabla\theta$ are available from the simulation of a turbulent reacting flow as a part of the solution $\theta = \theta(x,t)$. The transformation from empirical data $\theta(x,t)$ and their gradients $\nabla\theta$ to $\chi(\theta)$ plays a key role in transforming the iterative procedure applied to laminar steady flames [16] to the turbulent case.

Fig. 1 is a block diagram of the iterative methodology used here to provide gradient estimates for the REDIM table generation. At first, an initial manifold, boundary conditions and an initial guess for the gradient estimate are used to generate the REDIM table. This REDIM table is then used in reduced CFD calculations. Note that reduced CFD calculations here refer to the reacting flow simulations solving the transport equations for θ, instead of solving the transport equations for ψ, as explained in detail in Section 4. From these reduced CFD calculations, gradient data is extracted at some time steps of every two flow-through times. From these scattered data, gradient estimates for the REDIM method are calculated, as briefly explained in the next subsection. Also, at this step, the initial manifold for the next iteration step is calculated using the REDIM of the previous iteration step. Finally, if the convergence of the gradient estimates is achieved, the iterative loop stops, and the mean quantities are calculated in the reduced CFD calculations after a few flow-through times. The main advantage of

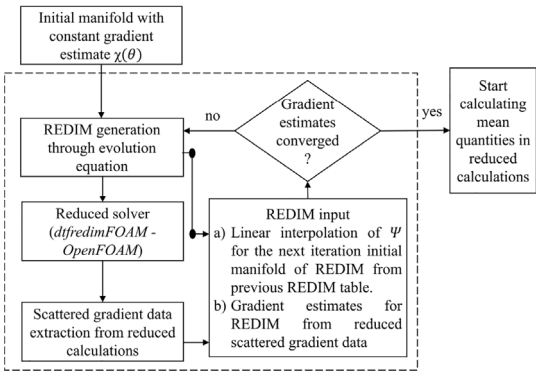

Fig. 1. Block diagram of an iterative procedure for REDIM table generation.

this approach is that it can provide a system-adapted REDIM without requiring any detailed calculations: The gradient information needed to construct the REDIM comes entirely from reduced calculations in the form of scattered data, which makes it independent of detailed calculations.

3.3. Gradient estimates method for REDIM

To create a REDIM gradient estimate from scattered gradient data, a variational (minimization) approach is used [16]. In this method, first, a function is created for an extensive scattering present in the gradient field using a weighted-interpolation approach. Afterwards, a smoothing operation is performed using a variational (minimization) approach that provides compensation between the smoothness and closeness of gradient estimates to scattered gradient data. The method can deliver smooth representations of the scattered gradient data, even if the data do not fully cover the whole state space. It also allows specifying boundary conditions on the edges of the state space domain. A detailed explanation of this method is given in [16].

From LES, $\chi(\theta)$ is approximated from the magnitude of the Favre-filtered spatial gradient field $|\nabla\tilde{\theta}| = |\widetilde{\nabla\theta}| \approx |\nabla\theta|$. In case of smaller SGS variance of θ, $\lim_{\widetilde{\theta''^2}\to 0}$, a linear variation of θ can be assumed over the smaller grid size [22]. For the current flame simulation calculation of $\widetilde{\theta''^2}$ by an algebraic model suggested in [22], shows the comparatively low value of $\widetilde{\theta''^2}$ relative to $\tilde{\theta}$. Therefore, this assumption should still be valid in the current flame simulation. To assess the influence of the spatial filtering involved in the LES simulations onto the gradient estimates, gradient estimates obtained from the LES were compared to the gradients of a (spatially better resolved) qDNS of the same flame [21].

Additionally, to address the issue of scatter in the data used for the gradient estimates, we perform conditional statistics on the gradients. The mean and standard deviation of $|\nabla\theta|$ are determined, conditioned on the values of θ. Small conditioned standard deviations signify that a good representation of the actual gradients by a function $\chi(\theta)$, which is the basic assumption of REDIM, is possible.

4. Turbulence/chemistry interaction

4.1. Thermo-kinetic coordinates based formulation

In order to simplify the reduced model formulation, the treatment of scatter and filtering issues as well as to avoid having to cope with gradients and divergences of generalized coordinates, a fixed parameterization is used here for the reduced variables in the REDIM model. For example, if $\psi = (h, p, Y_{\mathrm{CO_2}}, Y_{\mathrm{N_2}}, Y_{\mathrm{H}}, \ldots)^{\mathrm{T}}$, where h is the enthalpy, p the pressure and Y_r the mass fraction of species r, then a fixed parameterization can be chosen as $\theta \equiv \xi = (Y_{\mathrm{CO_2}}, Y_{\mathrm{N_2}})^T$. One only needs to make sure the parameterization is one-to-one with the given REDIM.

Note that a reduced equation formulation can also be implemented in generalized coordinates θ [13], where a projection based on the pseudo-inverse of ψ_θ, ψ_θ^+ is used. This ψ_θ^+ orthogonally projects diffusion, reaction and convection processes onto the tangential sub-space of the manifold, and it can be determined through different ways [23]. In the current formulation, a constant matrix-based parameterization projection, $\xi = C\psi$, is used. A detailed explanation and the difference between these two formulations is discussed in Refs. [14,16]. In particular, in [14], it was demonstrated that, once the REDIM is close to an invariant manifold, which is actually the case for the investigated problem, both formulations lead to equivalent solutions. The reduced transport equation for the thermo-kinetic coordinates k (ξ_k) can be determined from the original transport equation of ψ

$$\frac{\partial(\rho\xi_k)}{\partial t} + \nabla\cdot(\rho u\xi_k) = \nabla\cdot(D_{\xi_k}\nabla\xi_k) + \dot{\omega}_{\xi_k}, \tag{1}$$

where $k = 1, 2, \ldots, m_s$, and in case of 2D-REDIM $m_s = 2$. $\dot{\omega}_{\xi_k}$ is the source term of ξ_k. For unity Lewis number and equal mass diffusivity of species k, the diffusion coefficient is $D_{\xi_k} = D = \lambda/c_p$, where λ is the thermal conductivity and c_p is the specific heat capacity.

4.2. The DTF-REDIM model

The theoretical basis of the DTF model lies in premixed combustion [18,24]. However, it has been successfully used for simulating turbulent lifted [5], lean partially-premixed [25], and partially-premixed flames [6] before. A detailed description of the DTF model can be found in [17,19]. In the DTF-REDIM model, Eq. (1) is recast as:

$$\begin{aligned}\frac{\partial(\overline{\rho}\tilde{\xi}_k)}{\partial t} + \nabla\cdot\left(\overline{\rho}\tilde{u}\tilde{\xi}_k\right) = \nabla\cdot\Bigg(\Big\{ (E(Z)\mathcal{F}_{\mathrm{dyn},\xi}(Z) \\ D + (1-\Omega_\xi)D_t \Big\}\nabla\tilde{\xi}_k\Bigg) + \frac{E(Z)}{\mathcal{F}_{\mathrm{dyn},\xi}(Z)}\dot{\omega}(\tilde{\xi}_k),\end{aligned} \tag{2}$$

where symbol $\tilde{\cdot}$ represents the spatially filtered term. Unclosed terms for the reduced coordinates fluxes ($\widetilde{\rho u\xi_k} - \overline{\rho}\tilde{u}\tilde{\xi}_k$), which appear due to the filtering operation, are treated using a gradient-transport assumption [26], $\widetilde{\rho u\xi_k} - \overline{\rho}\tilde{u}\tilde{\xi}_k = -D_t\nabla\tilde{\xi}_k$. The eddy diffusivity D_t is the ratio of dynamic eddy viscosity (μ_t) to the turbulent Schmidt number (Sc_t), and in the current study Sc_t is set to 0.7.

A dynamic thickening factor as a function of mixture fraction (Z) is, $\mathcal{F}_{\mathrm{dyn},\xi}(Z) = 1 + \Omega_\xi(\mathcal{F}(Z) - 1)$, as in [19]. Where thickening factor $\mathcal{F}(Z) = \max\left(n_{gp}\Delta_m/\delta_L(Z), 1\right)$, flame sensor $\Omega_\xi = \tanh\left(5 * |\dot{\omega}_\xi|\right)$ and $\dot{\omega}_\xi$ is the source term of ξ. The number of grid points required to resolve the flame front (n_{gp}) is set to 5 [24], the mesh size (Δ_m) is approximated by the cubic root volume of the grid and δ_L is the laminar flame thickness, calculated as thermal flame thickness [18] within the flammability limit $0.035 \le Z \le 0.095$. The efficiency function ($E(Z)$) by [24] is used, with a constant model parameter $\beta = 0.5$. In the $E(Z)$, the laminar flame speed (s_L), calculated as in [18], is also a function of Z.

The Favre filtered equations for mass, momentum and reduced coordinates, Eq. (2), as well as an equation of state, are solved in the DTF-REDIM SGS model. The source terms for reduced coordinates ($\dot{\omega}(\tilde{\xi}_k)$), species mass fractions and temperature are taken from the REDIM chemistry table based on the ξ values. An additional table is provided which stores the δ_L and s_L values as a function of Z.

5. Numerical details

5.1. REDIM: Initial solution and gradient estimates

Fig. 2 shows the initial manifold in $\phi_{\mathrm{N_2}} - \phi_{\mathrm{CO_2}} - \phi_{\mathrm{CO}}$ state space projection, where ϕ is the specific mole number (ratio of mass fraction and molar mass) of the species. The solid red and blue lines represent the upper and lower boundaries, where the upper boundary consists of the Burke-Schumann solution [26], generated by 1-step chemistry, and

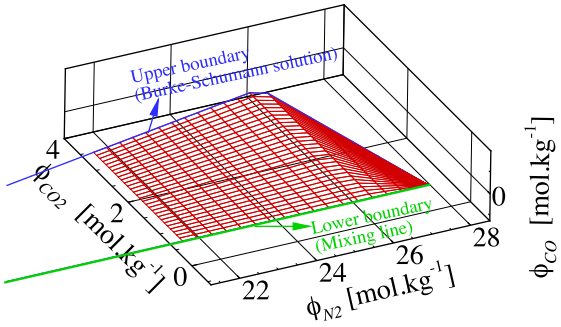

Fig. 2. The initial manifold used for generating the REDIM tables, viewed in $\phi_{N_2} - \phi_{CO_2} - \phi_{CO}$ space. Only part of the manifold is shown for better representation. The value of ϕ_{CO} is zero because the upper boundary is generated by 1-step chemistry which does not include any radicals or minor species.

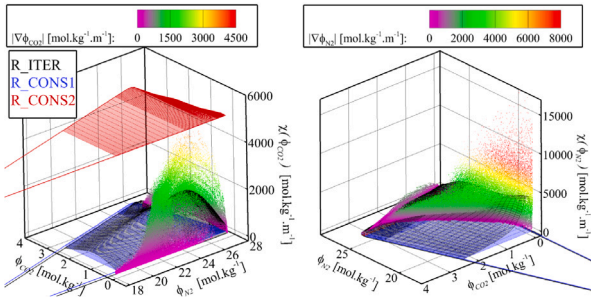

Fig. 3. Gradients obtained from the reduced calculation (scattered data), which are $|\nabla\phi_{CO_2}|$ and $|\nabla\phi_{N_2}|$, and corresponding gradient estimates $\chi(\phi_{CO_2})$ and $\chi(\phi_{N_2})$ in R_ITER (black mesh). Constant gradient estimates R_CONS1 (blue mesh) and R_CONS2 (red mesh) are also displayed. (For interpretation of the references to color in this figure legend, the reader is referred to the web version of this article.)

the lower boundary is made of a pure mixing line between the pure fuel to the pure air. This is a theoretical limit for accessible system states in the projected plane chosen for the constant parameterization. The in-between states of lower and upper boundaries are linearly interpolated. The initial grid points are 30 × 30, but in later REDIM integration time, these are increased to 90 × 90, as proposed in [27], such that the solution does not change with further improvement in the grid resolution. The GRI 3.0 detailed reaction mechanism provided the chemistry in the generation of REDIM [28].

In order to check the sensitivity of the REDIM with respect to the gradient estimates, three different types of reduced calculations are performed using three different types of REDIM: (1) In R_ITER, iterative gradient estimates are used, where initial gradient estimates are constant values, same as in R_CONS1 case, which is shown in the following; (2) In R_CONS1, constant gradient estimates $\chi(\phi_{N_2}) = 100$ mol/(kg m) and $\chi(\phi_{CO_2}) = 100$ mol/(kg m), are used; (3) In R_CONS2, constant gradient estimates $\chi(\phi_{N_2}) = 100$ mol/(kg m) and $\chi(\phi_{CO_2}) = 5000$ mol/(kg m), are used. For constant $\chi(\phi_{CO_2})$, the values 100 and 5000 are chosen because they are close to the minimum and maximum values, respectively, observed in the gradient data of ϕ_{CO_2}. Note that $\chi(\phi_{CO_2}) = 5000$ mol/(kg m) has been taken as an extreme value, which represents gradients obtained in a stoichiometric, premixed, freely propagating CH_4/air flame. This will clearly overestimate the gradients observed in the strained turbulent flame considered.

5.2. Computational domain and numerical settings

The present reduced LES computations are performed using the *dtfredimFOAM* solver implemented in the finite-volume open source code OpenFOAM [29]. The term μ_t is modeled by the WALE SGS turbulence model, based on previous work [21]. Temporal discretization is done by a second-order implicit Euler backward scheme. In case of spatial discretization, a second-order central difference scheme (CDS) for the diffusion term and a second-order CDS with a van Leer limiter for the convective term are used in the reduced coordinates transport equations. A second-order CDS with filtering high-frequency modes for the convective term in the momentum equation is used by a filtered linear scheme implemented in OpenFOAM, which is a low-dissipation scheme and provides a blending of upwind scheme up to 20%, depending on the ratio of the background (in-cell) gradient and face gradient. The magnitudes of gradients, used in the generation of REDIMs, are calculated explicitly using a second-order CDS, where the scattered data are extracted at the streamwise midplane of the computational domain. The time step size is limited to keep the maximum Courant number below 0.3.

The cylindrical computational domain length in the axial and radial directions is $50D$ and $7.5D$ respectively. A hexahedral mesh with non-uniform grid spacing is used, which has approximately 3.39 million cells. The smallest grid resolution in the radial direction is 0.127 mm, sufficiently resolving the shear layer between the jet and pilot, and the smallest axial grid resolution in the vicinity of the jet exit is 0.197 mm. Grid cells are stretched non-uniformly in radial and axial directions. The maximum and minimum ratios of Δ_m in the present LES to the qDNS within the axial locations $1 \leq x/D \leq 15$ and radial locations $0 \leq r/D \leq 3$ are approximately 6.62 and 3.03 respectively. The current grid resolution satisfies Pope's criterion for turbulent kinetic energy [30].

The fuel/air mixing chamber is not a part of the simulation; the main-jet inlet conditions coming from the mixing tube are taken from simulations of Zirwes et al. [21]. For the pilot and co-flow air, top-hat velocity profiles with $U_p = 26.6$ m/s and $U_c = 15$ m/s are used, respectively. The ξ components, Y_{CO_2} and Y_{N_2}, for the pilot are set to fixed value 0.1369 and 0.7238, resulting in a temperature $T_p = 2220$ K of the pilot. For co-flow air, they are also set to the fixed value $Y_{CO_2} = 0$ and $Y_{N_2} = 0.767$. The outlet and walls of the cylindrical domain are far from the region of interest. At the outlet, non-reflective boundary conditions for p and zero-gradient boundary conditions are used for other scalars. At the walls, no-slip boundary conditions for velocity and zero-gradient boundary conditions are used for other scalars. Furthermore, temporal statistics (time-averaged mean and RMS quantities, denoted by subscripts $Mean$ and RMS, respectively) are calculated for 10 flow-through times based on the main-jet velocity $(50D/U_j)$.

6. Results and discussion

6.1. Gradient estimates

Fig. 3 shows gradient fields (the magnitude of the gradients is shown) obtained from the final iteration of the reduced calculation (scattered data), and the devised gradient estimates ($\chi(\phi_{CO_2})$, $\chi(\phi_{N_2})$) in R_ITER (black mesh) for the REDIM at final iteration. Constant gradient estimates R_CONS1 (blue mesh) and R_CONS2 (red mesh) are also shown for comparison. The $\chi(\phi_{CO_2})$ obtained in R_ITER lie between the $\chi(\phi_{CO_2})$ for R_CONS1 and R_CONS2. Fig. 3 shows the smoothed weighted-interpolated gradient estimates on the REDIM mesh. Additionally, the red mesh illustrates the level of overestimation of the gradients used in R_CONS2 case. The LES involves spatial filtering, which tends to reduce the gradient magnitudes compared to their real values. This will affect the gradient estimate derived from the LES simulations. To quantify this deviation, the gradients derived from LES were compared to spatially better-resolved data from qDNS [21]. It was found that the LES-based gradients were by a factor of 2-3 below those of the qDNS. This factor can be considered small, given the low sensitivity of REDIMs with dimension two or higher with respect to the gradient estimate. The residuals of $\chi(\phi_{CO_2})$ and $\chi(\phi_{N_2})$ are also plotted at different steps of this iterative methodology in the supplementary

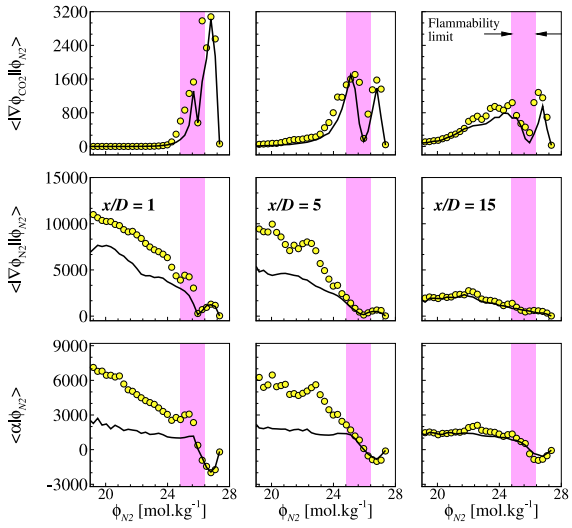

Fig. 4. Comparison of conditionally averaged ($\langle\,\rangle$) gradients obtained from qDNS (symbols) [21] and the final iteration step of reduced calculations of R_ITER (solid lines). Conditioning is on ϕ_{N_2}. Gradient magnitudes of ϕ_{CO_2} and ϕ_{N_2} are shown in rows 1 and 2, respectively. The bottom row shows the quantity $\alpha = \sqrt{|\nabla\phi_{CO_2} \cdot \nabla\phi_{N_2}|}\,\mathrm{sign}(\nabla\phi_{CO_2} \cdot \nabla\phi_{N_2})$. All gradient-related quantities are shown in mol/(kg m).

material (see Sec. S2), where residuals of $\chi(\phi_{CO_2})$ and $\chi(\phi_{N_2})$ show exponential convergence, and after the 3rd iteration, residuals do not change significantly.

Fig. 4 compares conditionally averaged ($\langle\,\rangle$) gradients obtained from the qDNS data (symbols) and from the final iteration of reduced calculations of R_ITER (solid lines) at three different axial locations. Conditioning is on ϕ_{N_2}, with an interval of 0.28. The magnitudes of gradients of ϕ_{CO_2} ($|\nabla\phi_{CO_2}|$) and ϕ_{N_2} ($|\nabla\phi_{N_2}|$) obtained from R_ITER show good qualitative agreement with qDNS, especially within the flammability limit used for this fuel/air mixture in [20]. The under-prediction of the gradients by R_ITER stems from the fact that in LES, spatial filtering reduces the magnitudes of gradients. For $\langle|\nabla\phi_{CO_2}||\phi_{N_2}\rangle$, gradients agree well with qDNS, however, $\langle|\nabla\phi_{N_2}||\phi_{N_2}\rangle$ profiles show higher discrepancies outside the flammability limits. Additionally, the quantity α (see caption of Fig. 4) representing the relation between gradients of CO_2 and N_2 is shown on the bottom row. The profiles of $\langle\alpha|\phi_{N_2}\rangle$ show good agreement with qDNS within the flammability limit.

6.2. Comparison of manifolds

Fig. 5 compares three different REDIMs, R_ITER, R_CONS1 and R_CONS2, together with conditionally averaged experimental data in Y_{N_2}-Y_{CO_2} space, color-coded with Y_{H_2O}. Black contour lines show the range of high T values. Conditional averaging of experimental data is performed with respect to Y_{N_2} and Y_{CO_2} after combining scattered data at different axial locations available in the experimental dataset. A significant difference between R_CONS2 and the other two REDIMs, as well as with a surface going through experimental data can be seen. Higher values of $\chi(\phi_{CO_2})$ in R_CONS2 lead to stronger diffusion in the Y_{CO_2} direction, causing higher values of Y_{H_2O} at states with comparatively low Y_{CO_2}. Note that significant differences are also observed near the right boundary of the manifold (large values of Y_{N_2}) for states corresponding to lean mixtures and describing processes of reaction and mixing with pure air. The R_ITER has $\chi(\phi_{CO_2})$ in between the R_CONS1 and R_CONS2 and the same can be seen in Fig. 5 for Y_{H_2O} values in the Y_{CO_2} directions. Similarly, in R_ITER, $\chi(\phi_{N_2})$ values are higher than in R_CONS1 and R_CONS2, also leading to more intense diffusion in the Y_{N_2} direction at the high T locations.

6.3. Comparison of radial profiles

A comparison of calculated and measured radial profiles for different scalars at different axial locations provides a better qualitative assessment of the simulation results than the comparison of different scalar fields. Fig. 6 compares measured and calculated mean and RMS radial statistics of Z, T, and Y_{CO_2} at four different axial locations. It can be seen that Z_{Mean}, T_{Mean} and $Y_{CO_2,Mean}$ quantities are well predicted by reduced calculations using REDIM at all the different axial locations. Although RMS quantities are slightly under-predicted at almost all the axial locations, the qualitative agreement is still good. It is also observed that both the mean and RMS profiles of R_ITER lie between R_CONS1 and R_CONS2, where, at the fuel-lean side, R_CONS2 and, at the fuel-rich side, R_CONS1 show good agreement with the measurement profiles.

The comparison demonstrates that even a rough gradient estimate is sufficient to create REDIMs of acceptable quality which reproduce the major species' "filtered" profiles and capture mixing *i.e.* diffusion processes. However, an accurate prediction of minor species like CO is a challenging task in the model reduction methods. Therefore, further comparison of the performance of current as well as flamelet-based approaches in terms of the prediction of CO is needed. To compare with flamelet-based methods, Favre mean radial profiles for Y_{CO} shown in [9,31] are used. In [9], premixed and non-premixed flamelet generated manifolds (FGM) are used in conjunction with Reynolds-averaged Navier–Stokes (RANS) based multi-environment probability density function (MEPDF) approach, and in [31], LES based non-premixed flamelet/progress-variable (FPV) and the premixed filtered tabulated chemistry LES (F-TACLES) models are used. However, the comparison shown here is only for qualitative purposes, since the grid quality, turbulent SGS closures, etc. vary in these simulations.

Fig. 7 shows the comparison of mean radial profiles of Y_{CO} obtained from different considered REDIMs, non-premixed FGM (F_NPFGM) [9], premixed FGM (F_PFGM) [9], non-premixed FPV (F_NPFPV) [31] and premixed F-TACLES (F_PF-TACLES) [31] with the measured values. The CO prediction using REDIM shows comparatively better agreement with measured values than it is shown in [9,31]. Also, note that in flamelet-based methods blending of the manifolds is needed for mixed-mode-based combustion [8] since premixed and non-premixed manifolds show a significant difference in the results. On the contrary, it is observed that the REDIM does not need the prior information for specific types of flamelets. Furthermore, a similar agreement for R_ITER is obtained for $Y_{CO,Mean}$ profiles as seen for other scalars in Fig. 6, where R_ITER profiles show in-between agreement compared with R_CONS1 and R_CONS2. Once one has an appropriate gradient estimation, *e.g.*, in the case R_CONS1, one might obtain reliable results. But if rough constant gradient estimation is used, *e.g.*, in the case R_CONS2, the quality of the reduced model might suffer either locally at some physical locations like in Fig. 7 shown by red lines or one might obtain under/overestimation of minor species. A similar observation is also noted for an OH radical (see supplementary material, Sec. S1). Nevertheless, R_ITER predicts the states of the qDNS with good accuracy. For instance, the conditionally averaged major species mass fractions of the qDNS in the Y_{N_2}-Y_{CO_2} space, were within 5% of the values predicted by the REDIM.

Hence, it is much better and safer to use the suggested iteration procedure, which adapts the estimate to the configuration and boundary conditions, and it requires a minimum prior knowledge about the combustion system. Moreover, in the implementation, it does not require (any) even one-dimensional (1D) integration of the detailed model.

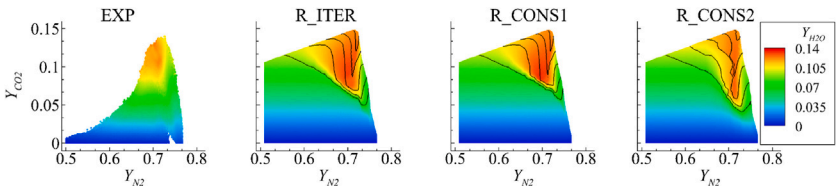

Fig. 5. Comparison of three REDIMs with conditionally averaged experimental data in Y_{N_2}-Y_{CO_2} space. Black contour lines show $1400 \leq T \leq 2200$ K. Only part of the manifold is shown.

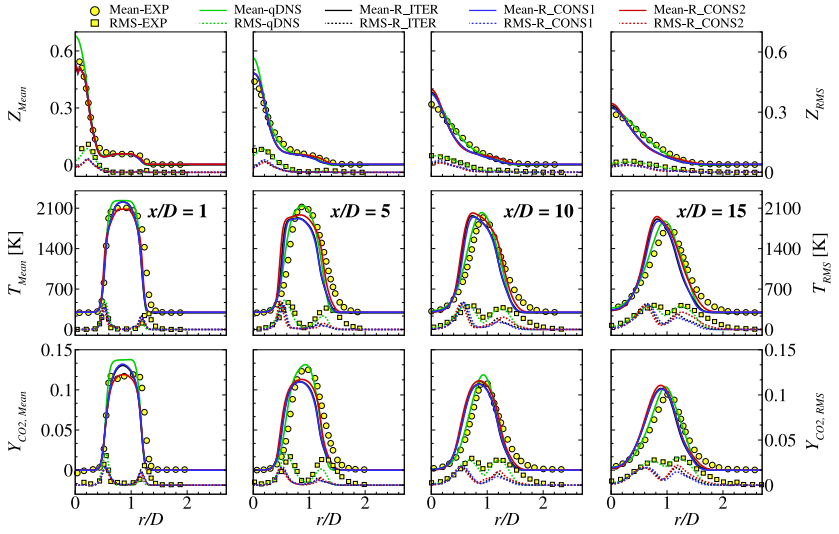

Fig. 6. Comparison of measured and calculated mean and RMS radial profiles of Z, T, and Y_{CO_2} at different axial locations.

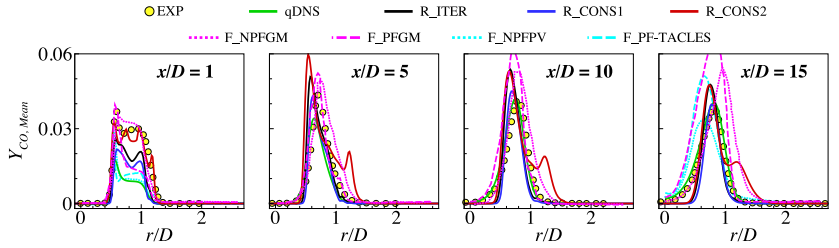

Fig. 7. Comparison of calculated mean radial profiles of Y_{CO} obtained from different considered REDIMs, non-premixed FGM (F_NPFGM) [9], premixed FGM (F_PFGM) [9], non-premixed FPV (F_NPFPV) [31] and premixed F-TACLES (F_PF-TACLES) [31] with measurement profiles at four different axial locations.

7. Conclusions

In the present work, LES of the Sydney turbulent partially-premixed flame with inhomogeneous inlets is performed using the DTF-REDIM SGS combustion model, where an iterative methodology is used to provide the gradient estimates to generate the REDIM table.

Three different reduced-chemistry LES calculations are performed using three different REDIMs, denoted here by R_ITER, R_CONS1 and R_CONS2. In R_ITER, an iterative approach is used to provide the gradient estimates to generate REDIM, while in R_CONS1 and R_CONS2, simplified constant gradient estimates are used to generate REDIMs. Comparison of radial statistics of mean and RMS scalar quantities predicted by reduced calculations using REDIMs show a good agreement with experimental and quasi-DNS (qDNS) datasets.

The iterative methodology for REDIM generation provides an improvement in model reduction methods when an *a priori* identification of the combustion system in terms of scalar-gradient correlations is difficult. Such cases can, for example, include partially-premixed combustion, which is studied in this work. In this methodology, the results of reduced calculations and the generation process of the REDIM are coupled to automatically adapt the REDIM to the gradient-scalar information from the simulation. The method, which has been applied to laminar flames in previous work [16], proved viable and efficient in the turbulent partially-premixed case of the present study. Notably, the REDIM proved to be rather robust against the spatial filtering operations of the LES, which tend to reduce the magnitude of the gradients in the simulations by a factor of 2–3 compared to their real values.

This observation corroborates that REDIMs of dimension two and higher depend only weakly on the gradient estimate, so that accuracy requirements on the gradient estimates for REDIM are very modest, and providing gradients with the correct order of magnitude may suffice in many practical cases. These observations, together with the inherent property of the REDIM model to allow freely adjustable dimension of the reduced model, make the automatic creation of reduced chemistry models for systems of arbitrary complex reaction–diffusion interaction realistic.

Novelty and significance statement

"On the fly"-method for creating reaction–diffusion manifolds (REDIM) for turbulent partially-premixed combustion with adaptation to the gradient-scalar correlations of the system. This approach, previously used in laminar steady flames, is now extended to turbulent combustion. It is significant because it makes the automatic creation of reduced chemistry models for systems with arbitrary complex reaction–diffusion interaction realistic.

CRediT authorship contribution statement

Prashant Shrotriya: Performed research, Analyzed data, Wrote the original draft of the paper. **Robert Schießl:** Designed research, Analyzed data, Reviewed and edited the paper. **Viatcheslav Bykov:** Designed research, Analyzed data, Reviewed and edited the paper. **Ulrich Maas:** Designed research, Analyzed data, Reviewed and edited the paper.

Declaration of competing interest

The authors declare that they have no known competing financial interests or personal relationships that could have appeared to influence the work reported in this paper.

Acknowledgments

The authors gratefully acknowledge Prof. A.R. Masri and Dr. R. Barlow for providing the experimental data, and Dr. T. Zirwes for providing the inlet boundary conditions and quasi-DNS (qDNS) dataset. This project received financial support from the German Research Foundation (DFG) within the projects SFB/TRR 150 (project number 237267381) within sub-project B06.

Appendix A. Supplementary data

Supplementary material related to this article can be found online at https://doi.org/10.1016/j.proci.2024.105273. Supplementary material is provided.

References

[1] A. Masri, Partial premixing and stratification in turbulent flames, Proc. Combust. Inst. 35 (2) (2015) 1115–1136.
[2] L.Y. Gicquel, G. Staffelbach, T. Poinsot, Large eddy simulations of gaseous flames in gas turbine combustion chambers, Prog. Energy Combust. Sci. 38 (6) (2012) 782–817.
[3] H. Pitsch, Large-eddy simulation of turbulent combustion, Annu. Rev. Fluid Mech. 38 (2006) 453–482.
[4] E. Knudsen, H. Pitsch, A general flamelet transformation useful for distinguishing between premixed and non-premixed modes of combustion, Combust. Flame 156 (3) (2009) 678–696.
[5] O. Schulz, T. Jaravel, T. Poinsot, B. Cuenot, N. Noiray, A criterion to distinguish autoignition and propagation applied to a lifted methane–air jet flame, Proc. Combust. Inst. 36 (2) (2017) 1637–1644.
[6] S. Popp, S. Hartl, D. Butz, D. Geyer, A. Dreizler, L. Vervisch, C. Hasse, Assessing multi-regime combustion in a novel burner configuration with large eddy simulations using tabulated chemistry, Proc. Combust. Inst. 38 (2) (2021) 2551–2558.
[7] B.A. Perry, M.E. Mueller, A.R. Masri, A two mixture fraction flamelet model for large eddy simulation of turbulent flames with inhomogeneous inlets, Proc. Combust. Inst. 36 (2) (2017) 1767–1775.
[8] K. Kleinheinz, T. Kubis, P. Trisjono, M. Bode, H. Pitsch, Computational study of flame characteristics of a turbulent piloted jet burner with inhomogeneous inlets, Proc. Combust. Inst. 36 (2) (2017) 1747–1757.
[9] N. Kim, Y. Kim, Multi-environment probability density function approach for turbulent partially-premixed methane/air flame with inhomogeneous inlets, Combust. Flame 182 (2017) 190–205.
[10] B. Fiorina, O. Gicquel, L. Vervisch, S. Carpentier, N. Darabiha, Approximating the chemical structure of partially premixed and diffusion counterflow flames using FPI flamelet tabulation, Combust. Flame 140 (3) (2005) 147–160.
[11] T. Zirwes, F. Zhang, P. Habisreuther, M. Hansinger, H. Bockhorn, M. Pfitzner, D. Trimis, Identification of flame regimes in partially premixed combustion from a quasi-DNS dataset, Flow Turbul. Combust. 106 (2021) 373–404.
[12] U. Maas, S.B. Pope, Implementation of simplified chemical kinetics based on intrinsic low-dimensional manifolds, Symp. (Int.) Combust. 24 (1) (1992) 103–112.
[13] V. Bykov, U. Maas, The extension of the ILDM concept to reaction–diffusion manifolds, Combust. Theory Model. 11 (6) (2007) 839–862.
[14] C. Strassacker, V. Bykov, U. Maas, Parametrization and projection strategies for manifold based reduced kinetic models, Proc. Combust. Inst. 37 (1) (2019) 763–770.
[15] Y. Luo, C. Strassacker, U. Maas, C. Hasse, Model reduction on the fly: Simultaneous identification and application of reduced kinetics for the example of flame-wall interactions, Proc. Combust. Inst. 39 (4) (2023) 5239–5248.
[16] P. Shrotriya, R. Schießl, C. Yu, V. Bykov, T. Zirwes, U. Maas, An iterative methodology for REDIM reduced chemistry generation and its validation for partially-premixed combustion, Combust. Theory Model. 28 (1) (2024) 65–98.
[17] J.-P. Legier, T. Poinsot, D. Veynante, Dynamically thickened flame LES model for premixed and non-premixed turbulent combustion, in: Proceedings of the Summer Program, 2000, pp. 157–168.
[18] S. Popp, G. Kuenne, J. Janicka, C. Hasse, An extended artificial thickening approach for strained premixed flames, Combust. Flame 206 (2019) 252–265.
[19] X. Wen, L. Dressler, A. Dreizler, A. Sadiki, J. Janicka, C. Hasse, Flamelet LES of turbulent premixed/stratified flames with H2 addition, Combust. Flame 230 (2021) 111428.
[20] R. Barlow, S. Meares, G. Magnotti, H. Cutcher, A. Masri, Local extinction and near-field structure in piloted turbulent CH4/air jet flames with inhomogeneous inlets, Combust. Flame 162 (10) (2015) 3516–3540.
[21] T. Zirwes, F. Zhang, P. Habisreuther, M. Hansinger, H. Bockhorn, M. Pfitzner, D. Trimis, Quasi-DNS dataset of a piloted flame with inhomogeneous inlet conditions, Flow Turbul. Combust. 104 (2020) 997–1027.
[22] J. Floyd, A.M. Kempf, A. Kronenburg 1, R. Ram, A simple model for the filtered density function for passive scalar combustion LES, Combust. Theory Model. 13 (4) (2009) 559–588.
[23] C. Yu, P. Shrotriya, U. Maas, Intrinsic low-dimensional manifold (ILDM)-based concept for the coupling of turbulent mixing with manifold-based simplified chemistry for the turbulent flame simulation, Phys. Fluids 34 (8) (2022).
[24] F. Charlette, C. Meneveau, D. Veynante, A power-law flame wrinkling model for LES of premixed turbulent combustion part I: Non-dynamic formulation and initial tests, Combust. Flame 131 (1–2) (2002) 159–180.
[25] P. Zhang, J.-W. Park, B. Wu, X. Zhao, Large eddy simulation/thickened flame model simulations of a lean partially premixed gas turbine model combustor, Combust. Theory Model. 25 (7) (2021) 1296–1323.
[26] J. Warnatz, U. Maas, R.W. Dibble, Combustion, fourth ed., Springer Berlin, Heidelberg, BW, 2006.
[27] C. Yu, U. Maas, Reaction-diffusion manifolds (REDIM) method for ignition by hot gas and spark ignition processes in counterflow flame configurations, Combust. Sci. Technol. 195 (10) (2023) 2400–2422.
[28] G.P. Smith, D.M. Golden, M. Frenklach, N.W. Moriarty, B. Eiteneer, M. Goldenberg, C.T. Bowman, R.K. Hanson, S. Song, W.C. Gardiner Jr., et al., GRI-Mech 3.0, 2022, http://combustion.berkeley.edu/gri-mech/version30/text30.html. (Accessed July 2022).
[29] H.G. Weller, G. Tabor, H. Jasak, C. Fureby, A tensorial approach to computational continuum mechanics using object-oriented techniques, Comput. Phys. 12 (6) (1998) 620–631.
[30] S.B. Pope, Turbulent Flows, Cambridge University Press, Cambridge, MA, 2000.
[31] H. Wu, M. Ihme, Compliance of combustion models for turbulent reacting flow simulations, Fuel 186 (2016) 853–863.